Bulletin of Mathematical Biology (2022) 84:5
https://doi.org/10.1007/s11538-021-00962-9

Society for Mathematical Biology

ORIGINAL ARTICLE

Dynamics of Stoichiometric Autotroph–Mixotroph–Bacteria Interactions in the Epilimnion

Yawen Yan[1] · Jimin Zhang[1,2] · Hao Wang[3]

Received: 6 July 2021 / Accepted: 25 October 2021

Abstract

Autotrophs, mixotrophs and bacteria exhibit complex interrelationships containing multiple ecological mechanisms. A mathematical model based on ecological stoichiometry is proposed to describe the interactions among them. Some dynamic analysis and numerical simulations of this model are presented. The roles of autotrophs and mixotrophs in controlling bacterioplankton are explored to examine the experiments and hypotheses of Medina–Sánchez, Villar–Argaiz and Carrillo for La Caldera Lake. Our results show that the dual control (bottom-up control and top-down control) of bacteria by mixotrophs is a key reason for the ratio of bacterial and phytoplankton biomass in La Caldera Lake to deviate from the general tendency. The numerical bifurcation diagrams suggest that the competition between phytoplankton and bacteria for nutrients can also be an important factor for the decrease of the bacterial biomass in an oligotrophic lake.

Keywords Stoichiometry · Autotrophs and mixotrophs · Bacteria · Bottom-up control · Top-down control

Yan and Zhang are supported by NSFC-11971088 and NSFHLJ-LH2021A003; Wang is supported by NSERC Discovery Grant RGPIN-2020-03911 and NSERC Accelerator Grant RGPAS-2020-00090.

✉ Jimin Zhang
zhangjm1978@hotmail.com

Yawen Yan
yywharbineu@163.com

Hao Wang
hao8@ualberta.ca

1 College of Mathematical Sciences, Harbin Engineering University, Harbin 150001, Heilongjiang, People's Republic of China

2 School of Mathematical Sciences, Heilongjiang University, Harbin 150080, Heilongjiang, People's Republic of China

3 Department of Mathematical and Statistical Sciences, University of Alberta, Edmonton, Alberta T6G 2G1, Canada

Published online: 22 November 2021

Mathematics Subject Classification 92D25 · 92B05 · 34A34

1 Introduction

Autotrophs (Autotrophic phytoplankton) and mixotrophs (mixotrophic phytoplankton) are two important components of phytoplankton in lakes. Autotrophs generally use photosynthesis to combine inorganic matters into organic matters for their own growth (Crane and Grover 2010; Stickney et al. 2000). Mixotrophs are the combination of autotrophic and heterotrophic nutrition, which can not only synthesize organic matters by photosynthesis, but also supply its own growth by ingesting bacteria and other microorganisms (Edwards 2019). Bacteria are also an important part of aquatic communities. They degrade organic matters and play indispensable roles in restoring water quality and maintaining the sustainable development of aquatic ecosystems (Chang et al. 2021; Grover 2003; Kong et al. 2018).

There are complex interactions between autotrophs, mixotrophs and bacteria with a variety of biological mechanisms (see Fig. 1). Nutrients and light are two essential resources for the growth of autotrophs (Chen et al. 2015; Yoshiyama and Nakajima 2002; Zhang et al. 2021). In the case of autotrophic nutrition, mixotrophs need to consume light and nutrients. This means that autotrophs and mixotrophs compete for light and nutrients (Moeller et al. 2019; Nie et al. 2019, 2020; Wilken et al. 2014a). In aquatic ecosystems, autotrophs and mixotrophs have an important impact on bacterial growth and biomass. First, autotrophs and mixotrophs release organic carbon through photosynthesis, which is an essential resource for bacterial growth (Edwards 2019; Wang et al. 2007). This creates a bottom-up control of bacteria. Second, mixotrophs in heterotrophic nutrition feed on bacteria and produce a top-down control for bacteria (Edwards 2019; Grover 2003). Third, the survival and reproduction of bacteria depend on organic carbon and nutrients (Crane and Grover 2010; Wang et al. 2007). This shows that there is a direct competition among autotrophs, mixotrophs and bacteria for nutrients. According to the above analysis, it is of great interest to propose a mathematical model to describe this complicated relationship among them. This is the original motivation of the paper.

Medina-Sánchez et al. (2004) evaluated the effects of biotic and abiotic factors on bacterioplankton production and biomass in La Caldera Lake, which is located in Spain. This lake is a high mountain lake with a surface area of 20,000 m^2. Its average water depth is 4.3 m (from 2 to 14 m), and nutrients are extremely scarce. Organic carbon is generated from phytoplankton photosynthesis, and the input of external organic carbon is negligible. Based on the data and experimental analysis from 1986 to 1999, they pointed out that phytoplankton were the most important factor for controlling bacterial biomass in this lake. Particularly, a top-down control of bacteria by mixotrophs was a key reason why the planktonic community of La Caldera Lake is different from the traditional tendency of a high ratio of bacterial to phytoplankton biomass in oligotrophic lakes. Another aim of this paper is to examine these experimental results theoretically via a mathematical model as describe above.

Ecological stoichiometry is a powerful tool for combining energy balance with multiple nutrients in an ecological system (Sterner and Elser 2002). Theoretical ecol-

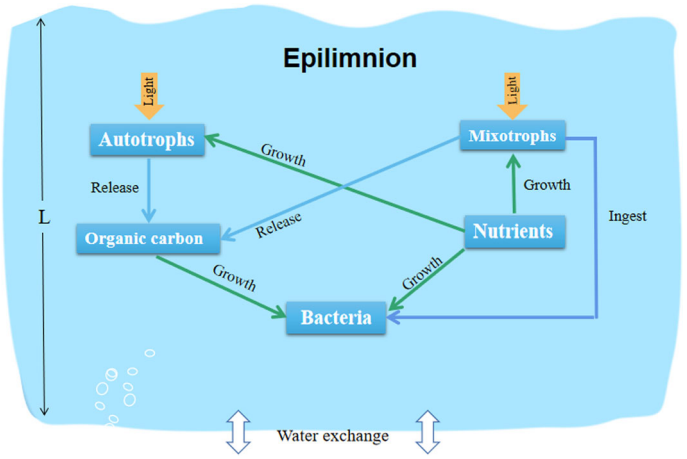

Fig. 1 (Color Figure Online) Autotroph–mixotroph–bacteria interactions in the epilimnion

ogy and experimental results have proved the importance of ecological stoichiometry. Models based on ecological stoichiometry are used to explore various ecological mechanisms and explain some existing paradoxes, such as producer–grazer systems (Li et al. 2011; Loladze et al. 2000; Peace and Wang 2019; Wang et al. 2008), three species model (Loladze et al. 2004; Peace 2015), plant and herbivore interactions (Rong et al. 2020), and organic matter decomposition (Kong et al. 2018; Wang et al. 2007). There is increasing recognition that phytoplankton including autotrophs and mixotrophs have varying nutrient/carbon ratios, which indicate their quality for zooplankton. It is thought to have important implications on the aquatic ecosystems (Loladze et al. 2000; Sterner and Elser 2002). In contrast, bacteria generally have a fixed ratio of nutrient/carbon. We will construct a stoichiometric model to explore autotroph–mixotroph–bacteria interactions.

Most lakes on the Earth have the phenomenon of stratification (Boehrer and Schultze 2008). Lakes are generally separated by a thermocline into two parts: epilimnion and hypolimnion (Boehrer and Schultze 2008; Zhang et al. 2021). Due to the abundant light and strong turbulence, the epilimnion is the upper warmer layer, which is usually well-mixed. The hypolimnion is the bottom colder layer which is usually dark and relatively undisturbed. Light from the surface of the lake gradually weakens with the increase of lake depth (Hsu and Lou 2010; Jiang et al. 2019; Peng and Zhao 2016; Wang et al. 2007). Nutrients from the bottom of the lake go through the hypolimnion and reach the epilimnion by water exchange (Wang et al. 2007; Zhang and Shi 2021; Zhang et al. 2018).

Autotroph–bacteria interactions in lakes have been modeled by many researchers (Heggerud et al. 2020; Wang et al. 2007). Various mathematical models have been developed to explore autotrophs and mixotrophs competition for nutrients or light in lakes (Moeller et al. 2019; Nie et al. 2019, 2020; Wilken et al. 2014a). To our knowledge, none of models consider autotroph–mixotroph–bacteria complex interactions (see Fig. 1). In view of the existing research and the above discussion, we will pro-

pose a mathematical model to characterize the interactions of autotrophs, mixotrophs and bacteria based on ecological stoichiometry. Our model extends, by incorporating mixotrophs, the work of Wang et al. (2007) where bacteria–algae interactions were modeled in the epilimnion.

The rest of the paper is organized as follows. In Sect. 2, we derive a stoichiometric model to explore the interactions of autotrophs, mixotrophs and bacteria in the epilimnion. In Sect. 3, we investigate the experiments and hypotheses of Medina-Sánchez, Villar-Argaiz and Carrillo in (Medina-Sánchez et al. 2004) based on this model. According to theoretical analysis and numerical simulations, we evaluate the roles of autotrophs and mixotrophs in controlling bacterioplankton in aquatic ecosystems by using the realistic environmental parameters. In the discussion section, we summarize our findings and state some questions for future study.

2 Derivation of the Model

We propose a stoichiometric model to describe the interactions of autotrophs, mixotrophs, bacteria, dissolved nutrients and dissolved organic carbon in the epilimnion. The epilimnion is generally a well-mixed layer due to turbulent diffusion effect (Huisman and Weissing 1994; Wüest and Lorke 2003; Yoshiyama and Nakajima 2002). Assume that x is the depth coordinate of the lake, $x = 0$ is the water surface and $x = L$ is the bottom of the epilimnion. Our model contains seven complex nonlinear ordinary differential equations, characterizing the rate of change for autotrophs (A), autotrophic cell quota (Q_a), mixotrophs (M), mixotrophic cell quota (Q_m), dissolved nutrients (N), bacteria (B) and organic carbon (C). All the variables and parameters with biological significance and realistic values of the model are listed in Table 1.

According to the Lambert-Beer law (Huisman and Weissing 1994), the light intensity at the depth x of a lake is

$$I(x, A, M) = I_{in} \exp\left(-K_{bg}x - (k_a A + k_m M)x\right), \ 0 < x < L.$$

The growth of autotrophs is assumed to be mainly dependent on dissolved nutrients N and light $I(x, A, M)$. The growth function of autotrophs takes the multiplication of a Monod form and a Droop form (Heggerud et al. 2020; Wang et al. 2007; Zhang et al. 2021) as

$$\mu_a(A, Q_a, M) = r_a \left(1 - \frac{Q_{\min,a}}{Q_a}\right) \bar{I}_a(A, M),$$

where

$$\bar{I}_a(A, M) = \frac{1}{L}\int_0^L \frac{I(x, A, M)}{I(x, A, M) + h_a} \mathrm{d}x = \frac{1}{W} \ln\left(\frac{I_{in} + h_a}{I(L, A, M) + h_a}\right),$$

Table 1 Variables and parameters with realistic values and biological significance of model (1)

Symbol	Meaning	Values	Units	Source
t	Time	Variables	Day	
x	Depth	Variables	m	
A	Biomass density of autotrophs	Variables	mgC/m^3	
Q_a	Autotrophic cell quota (N:C)	Variables	gN/gC	
M	Biomass density of mixotrophs	Variables	mgC/m^3	
Q_m	Mixotrophic cell quota (N:C)	Variables	gN/gC	
N	Dissolved nutrient concentration	Variables	mgN/m^3	
B	Biomass density of bacteria	Variables	mgC/m^3	
C	Dissolved organic carbon (DOC) concentration	Variables	mgC/m^3	
r_a	Maximum specific production rate of autotrophs	1	Day^{-1}	Crane and Grover (2010), Moeller et al. (2019)
r_m	Maximum specific production rate of mixotrophs	1	Day^{-1}	Crane and Grover (2010), Moeller et al. (2019)
r_b	Maximum growth rate of bacteria	2.5 (1.5–4)	Day^{-1}	Wang et al. (2007)
N_b	Nutrient input from the bottom	80 (0–150)	mgN/m^3	Wang et al. (2007)
$Q_{\min,a}$	Autotrophic cell quota at which growth ceases	0.004	gN/gC	Wang et al. (2007)
$Q_{\max,a}$	Autotrophic cell quota at which nutrient uptake ceases	0.04	gN/gC	Wang et al. (2007)
$Q_{\min,m}$	Mixotrophic cell quota at which growth ceases	0.001	gN/gC	Crane and Grover (2010)
$Q_{\max,m}$	Mixotrophic cell quota at which nutrient uptake ceases	0.01	gN/gC	Crane and Grover (2010)
δ_a	Maximum specific nutrient uptake rate of autotrophs	0.6 (0.2–1)	gN/gC/day	Wang et al. (2007)
δ_m	Maximum specific nutrient uptake rate of mixotrophs	0.6 (0.2–1)	gN/gC/day	Assumption
D	Water exchange rate	0.02	m/day	Wang et al. (2007)

Table 1 continued

Symbol	Meaning	Values	Units	Source
I_{in}	Light intensity at the water surface	300	μmol(photons)/(m^{2}s)	Wang et al. (2007)
K_{bg}	Background light attenuation coefficient	0.5 (0.3–0.9)	m^{-1}	Wang et al. (2007)
k_a	Light attenuation coefficient of autotrophs	0.0003	m^2/mgC	Wang et al. (2007)
k_m	Light attenuation coefficient of mixotrophs	0.0003	m^2/mgC	Assumption
h_a	Half-saturation constant for light-limited production of autotrophs	200	μmol(photons)/(m^{2}s)	Moeller et al. (2019)
h_m	Half-saturation constant for light-limited production of mixtotrophs	200	μmol(photons)/(m^{2}s)	Moeller et al. (2019)
l_a	Half-saturation constant for nutrient-limited production of autotrophs	1.5	mgN/m^3	Edwards (2019)
l_m	Half-saturation constant for nutrient-limited production of mixotrophs	1.5	mgN/m^3	Assumption
θ	Ratio of Bacterial to mixotrophic carbon in per cell	0.008	–	Edwards (2019)
δ	Half-saturation constant for bacterial ingestion	15	mgC/m^3	Assumption
q	Nutrient to carbon quota of bacteria	0.15	gN/gC	Wang et al. (2007)
a	Ingestion rate for bacteria	0.05	day^{-1}	Assumption
e	Conversion efficiency	0.6	–	Edwards (2019)
d_a	Loss rate of autotrophs	0.1–0.2	Day^{-1}	Crane and Grover (2010), Yoshiyama and Nakajima (2002)
d_m	Loss rate of mixotrophs	0.1–0.3	Day^{-1}	Crane and Grover (2010), Yoshiyama and Nakajima (2002)
d_b	Loss rate of bacteria	0.01-0.36	Day^{-1}	Edwards (2019); Wang et al. (2007)
v_a, v_m	Sinking velocity of autotrophs and mixotrophs respectively	0.1 (0.05–0.25)	m/day	Wang et al. (2007)
κ_n	Half-saturation constant for nutrient-limited production of bacteria	0.1 (0.06–0.4)	mgN/m^3	Wang et al. (2007)
κ_c	Half-saturation constant for DOC-limited production of bacteria	250 (100–400)	mgC/m^3	Wang et al. (2007)
γ	C-dependent yield constant for bacterial growth	0.5 (0.31-0.75)	–	Wang et al. (2007)
L	Depth of the eplimnion	4.3 (2–10)	m	Medina-Sánchez et al. (2004)

and $W = L(K_{bg} + k_a A + k_m M)$. Here $Q_{\min,a}$ is the minimum dissolved nutrient cell quota of autotrophs. The loss of autotrophic biomass density is $d_a A$ due to respiration, predation and death. In the bottom of the epilimnion, there are phytoplankton sinking and water exchange. Let v_a and D be the sinking rate and exchange rate, respectively. The nutrient uptake rate of autotrophs is $\rho_a(Q_a)g_a(N)$, where

$$\rho_m(Q_m) = \delta_m \frac{Q_{\max,m} - Q_m}{Q_{\max,m} - Q_{\min,m}}, \quad Q_{\min,m} \le Q_m \le Q_{\max,m},$$
$$g_m(N) = \frac{N}{l_m + N}.$$

The cell quota dilution rate of autotrophs is $\mu_a(A, Q_a, M)$.

Mixotrophs are a combination of autotrophic and heterotrophic nutrition (Edwards 2019). In autotrophic activities, the growth of mixotrophs also mainly depends on light and nutrient availability; thus, they compete with autotrophs. In heterotrophic situation, mixotrophs mainly ingest bacteria and sometimes a small amount of autotrophic organisms (Crane and Grover 2010; Moeller et al. 2019; Wilken et al. 2014a). To investigate the interactions between phytoplankton and bacteria, we here assume that mixotrophs only feed on bacteria in heterotrophic condition. The growth rate of mixotrophs is a complex function containing the light density $I(x, A, M)$, mixotrophic cell quota Q_m and heterotrophic bacteria B (Edwards 2019) as

$$\mu_m(A, M, Q_m, B) = \left(1 - \frac{Q_{\min,m}}{Q_m}\right)\left(r_m \bar{I}_m(A, M) + e\theta f(B)\right),$$

where

$$\bar{I}_m(A, M) = \frac{1}{L}\int_0^L \frac{I(x, A, M)}{I(x, A, M) + h_m} dx = \frac{1}{W} \ln\left(\frac{I_{in} + h_m}{I(L, A, M) + h_m}\right),$$
$$f(B) = \frac{aB}{\delta + B}.$$

Here $Q_{\min,m}$ is the minimum nutrient cell quota of mixotrophs, e is conversion efficiency, and θ is the ratio of bacterial to mixotrophic carbon in per cell.

The reduction of biomass of mixotrophs consists of three parts: lost biomass $d_m M$ due to death, respiration and predation, sinking biomass $v_m M/L$ and water exchange biomass DM/L. The absorption of dissolved nutrients of mixotrophs mainly comes from dissolved nutrients and heterotrophic bacteria. The mixotrophic nutrient uptake rate is $\rho_m(Q_m)g_m(N) + qf(B)$, where

$$\rho_m(Q_m) = \delta_m \frac{Q_{\max,m} - Q_m}{Q_{\max,m} - Q_{\min,m}}, \quad Q_{\min,m} \le Q_m \le Q_{\max,m}, \quad g_m(N) = \frac{N}{l_m + N}.$$

The cell quota dilution rate of mixotrophs is $\mu_m(A, M, Q_m, B)$.

The bacterial growth function depends on dissolved nutrients and organic carbon in the following form

$$g_b(N, C) = \frac{N}{\kappa_n + N}\frac{C}{\kappa_c + C}.$$

The reduction of bacterial biomass includes lost biomass $d_b B$ as death, respiration and grazing, water exchange biomass DB/L, and biomass $f(B)M$ of mixotroph predation.

The dissolved organic carbon (DOC) comes from the exudation of phytoplankton (autotrophs and mixotrophs) photosynthesis (Wang et al. 2007). It is expressed as

$$\mu_c(A, Q_a, M, Q_m) = r_a \frac{Q_{\min,a}}{Q_a} \bar{I}_a(A, M)A + r_m \frac{Q_{\min,m}}{Q_m} \bar{I}_m(A, M)M.$$

The reduction of dissolved organic carbon is decided by the consumption of bacteria $r_b g_b(N, C)B/\gamma$ and water exchange DC/L.

The change of dissolved nutrients N depends on consumption by autotrophs, mixotrophs and bacteria with consumption rate

$$\rho_a(Q_a)g_a(N)A + \rho_m(Q_m)g_m(N)M + q r_b g_b(N, C)B$$

and nutrient exchange $(D/L)(N_b - N)$ at the bottom of the epilimnion, where N_b is a fixed nutrient input concentration.

According to the above formulations, we obtain the following autotroph–mixotroph–bacteria interaction model:

$$\begin{aligned}
\frac{\mathrm{d}A}{\mathrm{d}t} &= \underbrace{\mu_a(A, Q_a, M)A}_{\text{growth of autotrophs}} - \underbrace{d_a A}_{\text{loss}} - \underbrace{\frac{v_a + D}{L}A}_{\text{sinking and exchange}},\\
\frac{\mathrm{d}Q_a}{\mathrm{d}t} &= \underbrace{\rho_a(Q_a)g_a(N)}_{\text{nutrient uptake of autotrophs}} - \underbrace{\mu_a(A, Q_a, M)Q_a}_{\text{dilution due to autotrophic growth}},\\
\frac{\mathrm{d}M}{\mathrm{d}t} &= \underbrace{\mu_m(A, M, Q_m, B)M}_{\text{growth of mixotrophs}} - \underbrace{d_m M}_{\text{loss}} - \underbrace{\frac{v_m + D}{L}M}_{\text{sinking and exchange}},\\
\frac{\mathrm{d}Q_m}{\mathrm{d}t} &= \underbrace{\rho_m(Q_m)g_m(N) + qf(B)}_{\text{nutrient uptake of mixotrophs}} - \underbrace{\mu_m(A, M, Q_m, B)Q_m}_{\text{dilution due to mixotrophic growth}},\\
\frac{\mathrm{d}N}{\mathrm{d}t} &= \underbrace{\frac{D}{L}(N_b - N)}_{\text{nutrient exchange}} - \underbrace{\rho_a(Q_a)g_a(N)A}_{\text{autotrophic consumption}} - \underbrace{\rho_m(Q_m)g_m(N)M}_{\text{mixotrophic consumption}} - \underbrace{q r_b g_b(N, C)B}_{\text{bacterial consumption}},\\
\frac{\mathrm{d}B}{\mathrm{d}t} &= \underbrace{r_b g_b(N, C)B}_{\text{bacterial growth}} - \underbrace{d_b B}_{\text{loss}} - \underbrace{\frac{D}{L}B}_{\text{exchange}} - \underbrace{f(B)M}_{\text{predation by mixotrophs}},\\
\frac{\mathrm{d}C}{\mathrm{d}t} &= \underbrace{\mu_c(A, Q_a, M, Q_m)}_{\text{DOC exudation from autotrophs and mixotrophs}} - \underbrace{\frac{1}{\gamma} r_b g_b(N, C)B}_{\text{consumption by bacteria}} - \underbrace{\frac{D}{L}C}_{\text{exchange}}.
\end{aligned} \tag{1}$$

Model (1) describes the complex interrelationships among autotrophs, mixotrophs and bacteria. If mixotrophs are not considered ($M = 0$ and $Q_m = 0$), model (1) will be transformed into a stoichiometric autotroph–bacteria interaction model, which is studied in (Wang et al. 2007).

In view of the biological meaning of (1), we will investigate the solutions of (1) with the initial values satisfying

$$\begin{aligned} &A(0) > 0,\ Q_{\min,a} \le Q_a(0) \le Q_{\max,a},\ M(0) > 0,\\ &Q_{\min,m} \le Q_m(0) \le Q_{\max,m},\ N(0) > 0,\ B(0) > 0,\ C(0) > 0. \end{aligned} \tag{2}$$

By using standard mathematical arguments, we conclude that for the initial values (2), (1) has a unique positive solution defined for all $t \ge 0$, and solutions with initial conditions in the set

$$\Omega := \left\{ (A, Q_a, M, Q_m, N, B, C) \in \mathbb{R}^7_+ \;\middle|\; \begin{array}{l} A \ge 0, M \ge 0, N \ge 0, B \ge 0, C \ge 0, \\ Q_{\min,a} \le Q_a \le Q_{\max,a},\ Q_{\min,m} \le Q_m \le Q_{\max,m} \end{array} \right\}$$

will remain there for all forward time.

In oligotrophic lake ecosystems, the general tendency is to have a high ratio of bacterial to phytoplankton biomass. However, Medina-Sánchez, Villar-Argaiz and Carrillo (Medina-Sánchez et al. 2004) found that this ratio shows the opposite trend in La Caldera Lake, and the similar phenomenon also appears in other middle and high latitude lakes. The possible factor for this phenomenon is the control of bacteria by autotrophs and mixotrophs. Especially, the dual control (bottom-up control and top-down control) of mixotrophs is a key reason for the planktonic community structure of La Caldera Lake.

In the following section, we will examine the above statements and hypotheses in (Medina-Sánchez et al. 2004) by using model (1). The reason for using model (1) is mainly based on the following considerations. Actual data in La Caldera Lake from 1986 to 1999 show that autotrophs, mixotrophs and bacteria have been interacting in aquatic communities, and the growth of bacteria depends on the release of organic carbon by photosynthesis of phytoplankton. This is in line with the assumptions of model (1). The nutrient input concentration is relatively low in the model, and only the epilimnion is considered. These are consistent with the fact that La Caldera Lake is an oligotrophic shallow lake. Therefore, model (1) can be well connected to aquatic ecosystems in La Caldera Lake.

3 Autotrophs and Mixotrophs Controlling Bacteria

In this section, we investigate the roles of autotrophs and mixotrophs in controlling bacterioplankton in lakes. There is a bounded set that attracts all solutions of (1) with initial conditions in Ω and system (1) is dissipative. The proof can be found in Appendix.

Theorem 1 *The set*

$$\Delta := \left\{ (A, Q_a, M, Q_m, N, B, C) \in \Omega \,\middle|\, \begin{array}{l} AQ_a + MQ_m + qB + N \le N_b, \\ C \le \frac{LN_b}{D}\left(\frac{r_a}{Q_{\min,a}} + \frac{r_m}{Q_{\min,m}}\right) \end{array} \right\}$$

is a globally attracting region, which means that system (1) *is dissipative.*

Model (1) is a very complex system such that it is difficult to describe its whole dynamic properties. In the following discussion, in order to examine experimental results and hypotheses in Medina-Sánchez et al. (2004), we will consider two subsystems: autotroph–bacteria model and mixotroph–bacteria model. By exploring the bacterial biomass in the two subsystems, we will evaluate the effect of autotrophs and mixotrophs in controlling bacterioplankton in lakes.

3.1 Autotroph–Bacteria Model

In the absence of mixotrophs, we consider the autotroph–bacteria interactions as a special case and choose

$$\mu_a(A, Q_a) = \mu_a(A, Q_a, 0) = r_a\left(1 - \frac{Q_{\min,a}}{Q_a}\right)\bar{I}_a(A, 0),$$
$$\mu_c(A, Q_a) = \mu_c(A, Q_a, 0, 0) = r_a\frac{Q_{\min,a}}{Q_a}\bar{I}_a(A, 0)A,$$

and model (1) reduces to

$$\begin{aligned} \frac{\mathrm{d}A}{\mathrm{d}t} &= \mu_a(A, Q_a)A - d_aA - \frac{v_a + D}{L}A, \\ \frac{\mathrm{d}Q_a}{\mathrm{d}t} &= \rho_a(Q_a)g_a(N) - \mu_a(A, Q_a)Q_a, \\ \frac{\mathrm{d}N}{\mathrm{d}t} &= \frac{D}{L}(N_b - N) - \rho_a(Q_a)g_a(N)A - qr_bg_b(N, C)B, \\ \frac{\mathrm{d}B}{\mathrm{d}t} &= r_bg_b(N, C)B - d_bB - \frac{D}{L}B, \\ \frac{\mathrm{d}C}{\mathrm{d}t} &= \mu_c(A, Q_a) - \frac{1}{\gamma}r_bg_b(N, C)B - \frac{D}{L}C. \end{aligned} \tag{3}$$

Wang et al. (2007) has investigated dynamics of model (3) and showed that (3) has three possible steady states as follows:
Nutrient-only steady state $E_1 = (0, Q_{a1}, N_b, 0, 0)$, where

$$Q_{a1} = \frac{r_aQ_{\min,a}(Q_{\max,a} - Q_{\min,a})\bar{I}_a(0, 0) + \delta_aQ_{\max,a}g_a(N_b)}{r_a(Q_{\max,a} - Q_{\min,a})\bar{I}_a(0, 0) + \delta_ag_a(N_b)}.$$

Autotroph–nutrient–organic carbon steady state $E_2 = (A_2, Q_{a2}, N_2, 0, C_2)$, where A_2, Q_{a2}, N_2, C_2 satisfy

$$\begin{aligned} &\mu_a(A, Q_a) - d_a - \frac{v_a + D}{L} = 0,\ \rho_a(Q_a)g_a(N) - \mu_a(A, Q_a)Q_a = 0, \\ &\frac{D}{L}(N_b - N) - \rho_a(Q_a)g_a(N)A = 0,\ \mu_c(A, Q_a) - \frac{D}{L}C = 0. \end{aligned} \tag{4}$$

Coexistence steady state $E_3 = (A_3, Q_{a3}, N_3, B_3, C_3)$, where $A_3, Q_{a3}, N_3, B_3, C_3$ satisfy

$$\begin{aligned} &\mu_a(A, Q_a) - d_a - \frac{v_a + D}{L} = 0,\ \rho_a(Q_a)g_a(N) - \mu_a(A, Q_a)Q_a = 0, \\ &\frac{D}{L}(N_b - N) - \rho_a(Q_a)g_a(N)A - qr_b g_b(N, C)B = 0, \\ &r_b g_b(N, C) - d_b - \frac{D}{L} = 0,\ \mu_c(A, Q_a) - \frac{1}{\gamma}r_b g_b(N, C) - \frac{D}{L}C = 0. \end{aligned} \tag{5}$$

We define the following critical values:

$$d_a^* := \mu_a(0, Q_{a1}) - \frac{v_a + D}{L},\ \ d_{b1} := r_b g_b(N_2, C_2) - \frac{D}{L}. \tag{6}$$

The threshold d_a^* represents the growth rate of autotrophs, which is related to the input nutrient concentration, water surface light intensity and minimum and maximum autotrophic cell quota. The threshold d_{b1} is the growth rate of bacteria when its growth depends on nutrient and organic carbon concentration. From Wang et al. (2007), the following conclusions hold:

1. E_1 always exists and is locally asymptotically stable if $d_a > d_a^*$;
2. E_2 exists and is unique if $0 < d_a < d_a^*$ and it is locally asymptotically stable if $d_b > d_{b1}$.

This indicates that d_a^* is a threshold for autotrophs to invade a lake, and d_{b1} is a threshold for bacteria to invade a lake in the presence of autotrophs.

We next establish the bifurcation of E_3 from E_2 at $d_b = d_{b1}$ using bifurcation theory (see (Crandall and Rabinowitz 1971, Theorem 1.7) and (Shi and Wang 2009, Theorem 3.3 and Remark 3.4)). The proof of the following theorem can be found in the Appendix.

Theorem 2 *If $0 < d_a < d_a^*$ holds, then*

(i) model (3) has at least one positive coexistence steady state E_3 for $0 < d_b < d_{b1}$;
(ii) near $(d_{b1}, A_2, Q_{a2}, N_2, 0, C_2)$, the set of the coexistence steady states is a smooth curve with a form $\{(d_{b1}(s), A_3(s), Q_{a3}(s), N_3(s), B_3(s), C_3(s)) : 0 < s < \delta_1\}$ for some $\delta_1 > 0$;

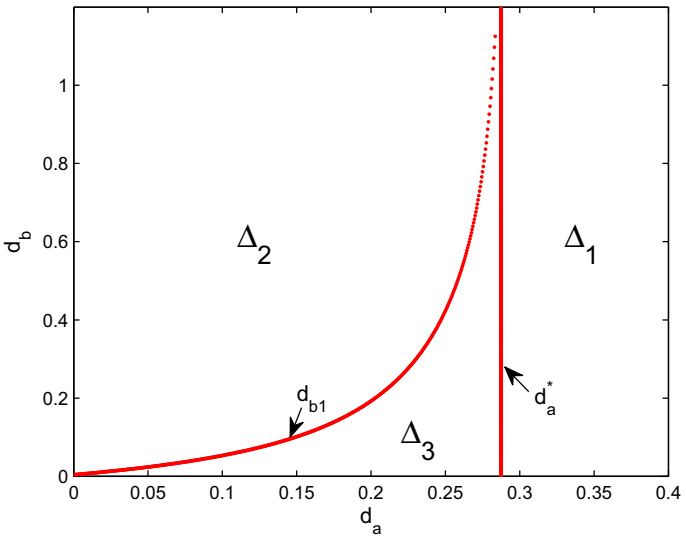

Fig. 2 Parameter ranges in the (d_a, d_b) plane with different extinction/existence scenarios. Δ_i, $i = 1, 2, 3$ are defined in (7), d_a^* is a critical threshold for autotroph invasion, and d_{b1} is a critical threshold for bacteria invasion when autotrophs exist. Here the rest parameter values are from Table 1

According to the above model analysis, we divide the parameters (d_a, d_b) plane as follows:

$$\begin{aligned} \Delta_1 &:= \{(d_a, d_b) : d_a > d_a^*\}, \\ \Delta_2 &:= \{(d_a, d_b) : 0 < d_a < d_a^*,\ d_b > d_{b1}\}, \\ \Delta_3 &:= \{(d_a, d_b) : 0 < d_a < d_a^*,\ 0 < d_b < d_{b1}\}. \end{aligned} \tag{7}$$

As a result of the presence of N_b, the system will not be completely extinct. The extinction of autotrophs and bacteria is inevitable if the autotrophic loss rate d_a is larger than d_a^*, regardless of the value of d_b (see Δ_1 in Fig. 2). Theoretical analysis and numerical simulations also indicate that E_1 is stable for (3) in Δ_1. This is because the organic carbon released by photosynthesis of autotrophs is a essential resource for the bacterial growth. Hence, the extinction of autotrophs will cause the extinction of bacteria. This means that autotrophs have a bottom-up control of bacteria.

Autotrophs, nutrients and organic carbon can coexist in a lake if the loss rate of bacteria is large (see Δ_2 in Fig. 2). In this case, E_2 is stable in the region Δ_2. From (4), (6) and Fig. 2, d_{b1} is a strictly monotone increasing function with respect to d_a. This shows that the decrease of the biomass of autotrophs is conducive to the invasion of bacteria into the lake when autotrophs exist. Autotrophs and bacteria can appear together in Δ_3 for two different cases. The first case is that the two coexist in a positive steady state E_3 (see Theorem 2 and $d_a \in (0.077, 0.138) \cup (0.252, 0.287)$ in Fig. 3). It is not known whether E_3 is unique and stable although it is confirmed by numerical simulations. The second case is that they coexist at a periodic solution (see $d_a \in (0.138, 0.252)$ in Fig. 3). Bacterial biomass and autotrophic biomass exhibit

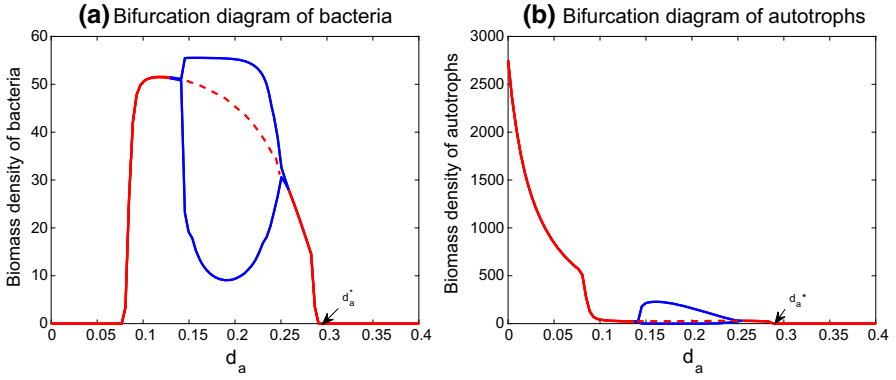

Fig. 3 Bifurcation diagrams of bacteria and autotrophs for $d_a \in (0, 0.4)$ and $d_b = 0.04$. Figures show the influence of autotrophic biomass density changes on bacterial biomass density by a bottom-up control and competition. Here the rest parameter values are from Table 1

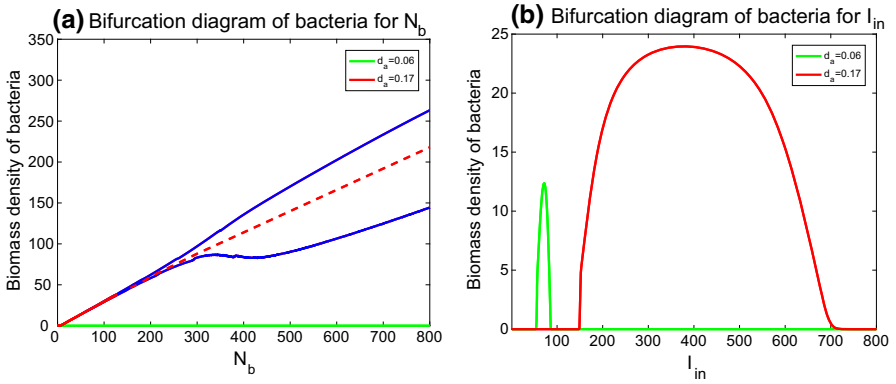

Fig. 4 Bifurcation diagrams of bacteria for $N_b \in (0, 800)$ and $I_{in} \in (0, 800)$. The results show the effects of abiotic factors (the water surface light intensity and nutrient input concentration) on bacterial biomass for the autotrophic loss rate $d_a = 0.06$ or $d_a = 0.17$. Here $d_b = 0.08$ and the rest parameter values are from Table 1

periodic oscillations. It is consistent with the findings in Wang et al. (2007). In Fig. 3, the numerical bifurcation diagrams imply that E_3 has two stability switches for the autotrophic loss rate d_a.

In model (3), the nutrient input concentration N_b and the water surface light intensity I_{in} are two important abiotic factors. Figure 4a shows that the high nutrient input concentration is beneficial to improve the bacterial biomass for the autotrophic loss rate $d_a = 0.17$. The reason for this phenomenon is that high nutrient concentration can weaken the competition between autotrophs and bacteria for nutrients, which leads to the increase of the bacterial biomass. If the biomass of autotrophs is relatively high ($d_a = 0.06$), it is difficult to raise the bacterial biomass with the increase of the nutrient concentration. This indicates that the competition between autotrophs and bacteria for nutrients directly affects the bacterial biomass in oligotrophic aquatic ecosystems.

Only moderate light intensity is conducive to the growth of bacteria. The lower and higher light intensities are harmful to bacteria (see Fig. 4b). This is because organic carbon and nutrients are two essential resources for the bacterial growth. The lower light intensity reduces organic carbon production in autotrophs. On the contrary, the higher light intensity causes a rapid increase in the biomass of autotrophs, which consumes more nutrients.

From Figs. 2 and 3, one can observe the extinction of bacteria for the smaller or larger d_a. The organic carbon released by autotrophs is an essential resource for the survival of bacteria, thus forming a bottom-up control of bacteria. The larger d_a would lead to the death of autotrophs and then cause the extinction of bacteria. Another different scenario is the smaller d_a. In this situation, the biomass of autotrophs increases drastically. Although autotrophs produce more organic carbon for the bacterial growth, it also consumes a great quantity of nutrients, which are another essential resource for bacteria to survive. Therefore, the principle of competition exclusion holds, and it is likely to cause the extinction of bacteria. It can be seen from the above discussion that the bacterial biomass is more sensitive to the biomass change of autotrophs than abiotic factors. From Fig. 4a, in an oligotrophic lake, the competition between autotrophs and bacteria for nutrients may also be one of important reason for the decrease of the bacterial biomass.

3.2 Mixotroph–Bacteria Model

In the absence of autotrophs, we consider the mixotroph–bacteria interactions as a special case and choose

$$\mu_m(M, Q_m, B) = \mu_m(0, M, Q_m, B) = \left(1 - \frac{Q_{\min,m}}{Q_m}\right)\left(r_m \bar{I}_m(0, M) + e\theta f(B)\right),$$
$$\mu_c(M, Q_m) = \mu_c(0, 0, M, Q_m) = r_m \frac{Q_{\min,m}}{Q_m} \bar{I}_m(0, M)M.$$

Model (1) transforms into

$$\begin{aligned}
\frac{\mathrm{d}M}{\mathrm{d}t} &= \mu_m(M, Q_m, B)M - d_m M - \frac{v_m + D}{L}M,\\
\frac{\mathrm{d}Q_m}{\mathrm{d}t} &= \rho_m(Q_m)g_m(N) + qf(B) - \mu_m(M, Q_m, B)Q_m,\\
\frac{\mathrm{d}N}{\mathrm{d}t} &= \frac{D}{L}(N_b - N) - \rho_m(Q_m)g_m(N)M - qr_b g_b(N, C)B,\\
\frac{\mathrm{d}B}{\mathrm{d}t} &= r_b g_b(N, C)B - d_b B - \frac{D}{L}B - f(B)M,\\
\frac{\mathrm{d}C}{\mathrm{d}t} &= \mu_c(M, Q_m) - \frac{1}{\gamma}r_b g_b(N, C)B - \frac{D}{L}C.
\end{aligned} \tag{8}$$

Compared with the model (3), the relationship between mixotrophs and bacteria is more complicated. Mixotrophs release organic carbon by photosynthesis in

autotrophic conditions to support the growth of bacteria, and they compete for nutrients. In heterotrophic cases, mixotrophs feed on bacteria.

We investigate the existence and local stability of boundary and positive steady states of (8). The possible steady states of (8) are listed below:
Nutrient-only steady state $E_4 = (0, Q_{m4}, N_b, 0, 0)$, where

$$Q_{m4} = \frac{r_m Q_{\min,m}(Q_{\max,m} - Q_{\min,m})\bar{I}_m(0,0) + \delta_m Q_{\max,m} g_m(N_b)}{r_m(Q_{\max,m} - Q_{\min,m})\bar{I}_m(0,0) + \delta_m g_m(N_b)}.$$

Mixotroph–nutrient–organic carbon steady state $E_5 = (M_5, Q_{m5}, N_5, 0, C_5)$, where M_5, Q_{m5}, N_5, C_5 solve

$$\begin{aligned} &\mu_m(M, Q_m, 0) - d_m - \frac{v_m + D}{L} = 0,\ \rho_m(Q_m)g_m(N) - \mu_m(M, Q_m, 0)Q_m = 0,\\ &\frac{D}{L}(N_b - N) - \rho_m(Q_m)g_m(N)M = 0,\ \mu_c(M, Q_m) - \frac{D}{L}C = 0. \end{aligned} \tag{9}$$

Coexistence steady state $E_6 = (M_6, Q_{m6}, N_6, B_6, C_6)$, where $M_6, Q_{m6}, N_6, B_6, C_6$ solve

$$\begin{aligned} &\mu_m(M, Q_m, B) - d_m - \frac{v_m + D}{L} = 0,\\ &\rho_m(Q_m)g_m(N) + qf(B) - \mu_m(M, Q_m, B)Q_m = 0,\\ &\frac{D}{L}(N_b - N) - \rho_m(Q_m)g_m(N)M - qr_b g_b(N, C)B = 0,\\ &r_b g_b(N, C)B - d_b B - \frac{D}{L}B - f(B)M = 0,\\ &\mu_c(M, Q_m) - \frac{1}{\gamma}r_b g_b(N, C)B - \frac{D}{L}C = 0. \end{aligned}$$

We let

$$d_m^* := \mu_m(0, Q_{m4}, 0) - \frac{v_m + D}{L},\ d_{b2} := r_b g_b(N_5, C_5) - \frac{D}{L} - \frac{aM_5}{\delta}. \tag{10}$$

The quantity d_m^* describes the growth rate of mixotrophs. It is related to the nutrient input concentration, light intensity and mixotrophic cell quota. The quantity d_{b2} is the growth rate of bacteria containing nutrients, organic carbon and mixotrophs.

The following result determines the existence and stability of E_4, E_5 and E_6. The proof can be found in the Appendix.

Theorem 3 *(i) E_4 always exists and it is locally asymptotically stable if $d_m > d_m^*$;*
(ii) E_5 exists and is unique if $0 < d_m < d_m^*$ and it is locally asymptotically stable if $d_b > d_{b2}$;
(iii) Assume that $0 < d_m < d_m^*$. Then model (8) has at least one positive coexistence steady state E_6 for $0 < d_b < d_{b2}$;

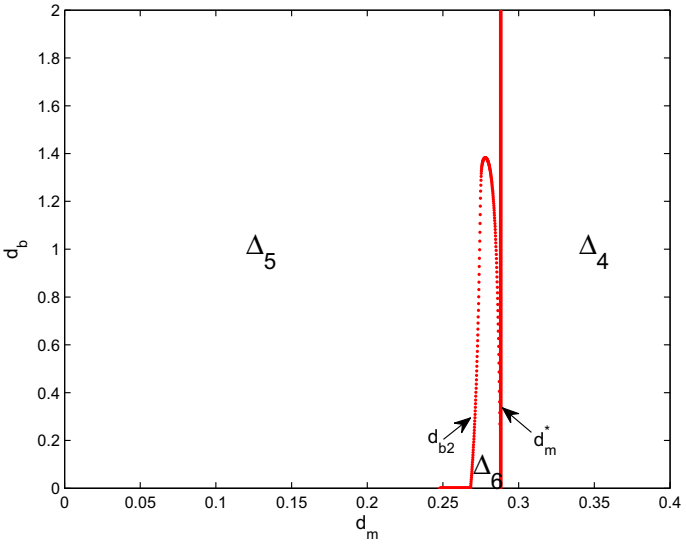

Fig. 5 Parameter ranges in the (d_m, d_b) plane with different extinction/existence scenarios. $\Delta_i, i = 4, 5, 6$ are defined in (11), d_m^* is a critical threshold for mixotroph invasion, and d_{b2} is a critical threshold for bacteria invasion when mixotrophs exist. Here the rest parameter values are from Table 1

(iv) Near $(d_{b2}, M_5, Q_{m5}, N_5, 0, C_5)$*, the set of the coexistence steady states is a smooth curve with a form* $\{(d_b(s), M_6(s), Q_{m6}(s), N_6(s), B_6(s), C_6(s)) : 0 < s < \delta_2\}$ *for some* $\delta_2 > 0$.

Theorem 3 shows that d_m^* and d_{b2} are the critical values for mixotrophs and bacteria in the epilimnion from extinction to survival respectively. Compared with the expression of d_{b1} in (6), there is one more term aM_5/δ in d_{b2}. It is caused by mixotrophs ingesting bacteria. Hence, mixotrophs have a top-down control of bacteria. This indicates that bacteria are more difficult to invade the aquatic system due to the influence of mixotrophs on bacterial predation.

For the convenience of the following discussion, the parameter space of (d_m, d_b) is partitioned into the following regions according to Theorem 3 (see Fig. 5):

$$\begin{aligned} \Delta_4 &:= \{(d_m, d_b) : d_m > d_m^*\}, \\ \Delta_5 &:= \{(d_m, d_b) : 0 < d_m < d_m^*,\ d_b > d_{b2}\}, \\ \Delta_6 &:= \{(d_m, d_b) : 0 < d_m < d_m^*,\ 0 < d_b < d_{b2}\}. \end{aligned} \tag{11}$$

During autotrophic activities, mixotrophs release organic carbon by photosynthesis to support the bacterial growth. It reveals a bottom-up control of bacteria by mixotrophs. If mixotrophs are extinct, bacteria will not survive. Therefore, only if the loss rate of mixotrophs is greater than d_m^*, solutions of (8) converge to E_4 in the region Δ_4 (see (i) in Theorem 3). Conclusion (ii) in Theorem 3 shows that E_5 is stable in the region Δ_5. This means that mixotrophs, nutrients and organic carbon can coexist in an aquatic ecosystem. Theorem 3 and numerical bifurcation diagrams show that mixotrophs and

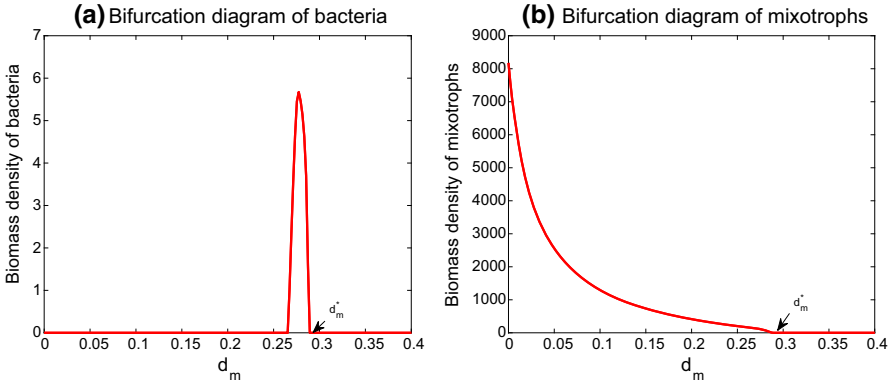

Fig. 6 Bifurcation diagrams of bacteria and mixotrophs for $d_m \in (0, 0.4)$ and $d_b = 0.04$. Figures show the influence of mixotrophic biomass density changes on bacterial biomass density by a dual control and competition. Here the rest parameter values are from Table 1

bacteria can also coexist in a stable positive steady state E_6 or a positive periodic solution in Δ_6. Note that mixotrophs and bacteria directly compete for nutrients; the low loss rate of mixotrophs causes a rapid decrease of bacterial biomass, or even extinction (see Fig. 6).

By comparing the effects of autotrophs and mixotrophs on bacteria in the autotroph–bacteria model and the mixotroph–bacteria model, it is found that there are similarities as well as many differences between them. They all have a bottom-up control of bacteria through the organic carbon released by photosynthesis. The result of this control is that the extinction of autotrophs and mixotrophs will inevitably bring about the extinction of bacteria (see Δ_1 in Fig. 2 and Δ_4 in Fig. 5). Because of the direct competition for nutrients, the lower loss rate of autotrophs or mixotrophs will cause the extinction of bacteria (see Δ_2 in Fig. 2 and Δ_5 in Fig. 5). Autotrophs and bacteria or mixotrophs and bacteria can coexist in lakes, but there are differences between the two coexistence. One difference is the parameter range of bacterial survival. The loss rate range of bacterial survival in the model (8) is much smaller than that in the model (3) (see Δ_3 in Fig. 2 and Δ_6 in Fig. 5). Another difference is the bacterial biomass. From (a) in Figs. 3 and 6, bacteria in the model (3) exhibit strong periodic oscillation and higher biomass compared to the model (8). The main reason for the above differences is the predation effect of mixotrophs on bacteria, which produces a top-down control.

The growth of autotrophs generally declines sharply in winter or under oligotrophic conditions. But mixotrophs exhibit better adaptability due to heterotrophic activities. Even when the light intensity and nutrients are insufficient, they can still survive by preying on bacteria. La Caldera Lake is an oligotrophic high mountain lake. This makes mixotrophs to obtain an advantage in the competition with autotrophs and to occupy a dominant position through heterotrophic effects within a certain period of time. Compared with the theoretical analysis and numerical simulations of models (3) and (8), it is found that the top-down control of bacteria by mixotrophs makes an obvious difference between the two models and significantly reduces the bacterial

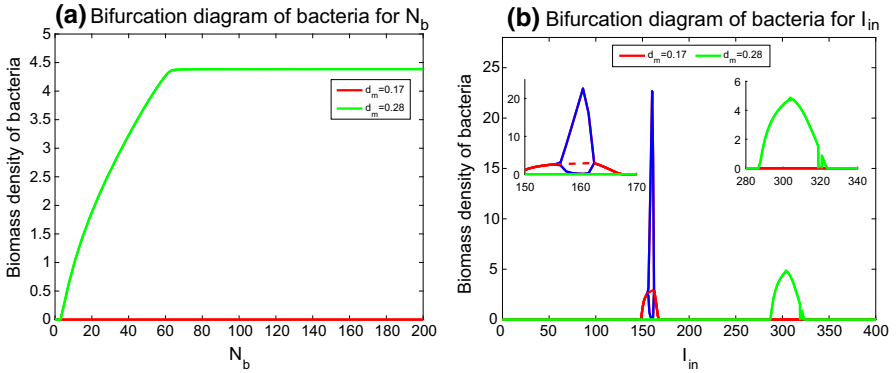

Fig. 7 Bifurcation diagrams of bacteria for $N_b \in (0, 200)$ and $I_{in} \in (0, 400)$. The results show the effects of abiotic factors on bacterial biomass for the mixtotrophic loss rate $d_m = 0.17$ or $d_m = 0.28$. Here $d_b = 0.08$ and the rest parameter values are from Table 1

biomass. This also shows that the top-down control is a key factor for the composition of phytoplankton and bacteria in La Caldera Lake.

We now explore the influence of N_b and I_{in} on the bacterial biomass in the model (8). From Fig. 7, it can be observed that the phenomenon similar to Fig. 4 is that the increase in the input nutrient concentration and the moderate light intensity are beneficial to the bacterial growth. As a result of the predation of bacteria by mixotrophs and their competition for nutrients, the high biomass of mixotrophs can cause the extinction of bacteria even if the nutrients are abundant (see $d_m = 0.17$ in Fig. 7a). An interesting observation is that the bacterial biomass remains unchanged when the nutrient input concentration reaches a certain value (see $d_m = 0.28$ in Fig. 7a). This is mainly caused by the predator of mixotrophs on bacteria, resulting in a top-down control.

In the models (3) and (8), we explore the influence of autotrophs and mixotrophs in controlling bacterioplankton respectively. From Figs. 3 and 6, one can also observe that the biomass of bacteria is very sensitive to the change of the biomass of autotrophs or mixotrophs near the thresholds. The small change for the biomass of autotrophs or mixotrophs will have a greater impact on the bacterial biomass. The theoretical analysis and numerical simulations in the models (3) and (8) indicate that both autotrophs and mixotrophs can reduce the bacterial biomass through a bottom-up control. In particular, the dual control (bottom-up control and top-down control) of mixotrophs has a more obvious effect on the bacterial biomass because of the predation of mixotrophs on bacteria. This implies that the role of mixotrophs is more prominent in reducing the bacterial biomass.

3.3 Autotroph–Mixotroph–Bacteria Model

The interactions among autotrophs, mixotrophs and bacteria are extremely complex including competition and predation, bottom-up and top-down control. It is challenging to characterize the complete dynamic properties of model (1). Here we only describe the existence and local stability of steady states of (1). Model (1) may have

seven steady states:

$$e_1 = (0, Q_{a1}, 0, Q_{m1}, N_b, 0, 0),\ e_2 = (A_2^*, Q_{a2}^*, 0, Q_{m2}^*, N_2^*, 0, C_2^*),$$
$$e_3 = (0, Q_{a3}^*, M_3^*, Q_{m3}^*, N_3^*, 0, C_3^*),\ e_4 = (A_4^*, Q_{a4}^*, M_4^*, Q_{m4}^*, N_4^*, 0, C_4^*),$$
$$e_5 = (A_5^*, Q_{a5}^*, 0, Q_{m5}^*, N_5^*, B_5^*, C_5^*),\ e_6 = (0, Q_{a6}^*, M_6^*, Q_{m6}^*, N_6^*, B_6^*, C_6^*),$$
$$e_7 = (A_7^*, Q_{a7}^*, M_7^*, Q_{m7}^*, N_7^*, B_7^*, C_7^*).$$

We consider the following critical death rates:

$$d_{a1}^* := \mu_a(0, Q_{a3}^*, M_3^*) - \frac{v_a + D}{L},\ d_{a2}^* := \mu_a(0, Q_{a6}^*, M_6^*) - \frac{v_a + D}{L},$$
$$d_{m1}^* := \mu_m(A_2^*, 0, Q_{m2}^*, 0) - \frac{v_m + D}{L},\ d_{m2}^* := \mu_m(A_5^*, 0, Q_{m5}^*, 0) - \frac{v_m + D}{L},$$
$$d_{b1}^* := r_b g_b(N_2^*, C_2^*) - \frac{D}{L},\ d_{b2}^* := r_b g_b(N_3^*, C_3^*) - \frac{D}{L} - \frac{aM_3^*}{\delta},$$
$$d_{b3}^* := r_b g_b(N_4^*, C_4^*) - \frac{D}{L} - \frac{aM_4^*}{\delta}.$$

By using similar arguments to those in Theorems 2 and 3, we will show the coexistence and local stability of boundary steady states of (1).

Theorem 4 (i) *The nutrient-only steady state e_1 always exists and it is locally asymptotically stable if $d_a > d_a^*, d_m > d_m^*$, where d_a^*, d_m^* are given in (6) and (10);*

(ii) *The autotroph-only steady state e_2 exists and is unique if $0 < d_a < d_a^*$ and it is locally asymptotically stable if $d_m > d_{m1}^*,\ d_b > d_{b1}^*$; The mixotroph-only steady state e_3 exists and is unique if $0 < d_m < d_m^*$ and it is locally asymptotically stable if $d_a > d_{a1}^*,\ d_b > d_{b2}^*$;*

(iii) *Model (1) has at least one autotroph–mixotroph-only steady state e_4 if $0 < d_a < d_{a1}^*,\ 0 < d_m < d_{m1}^*$, one autotroph–bacteria-only steady state e_5 if $0 < d_a < d_a^*,\ 0 < d_b < d_{b1}^*$, and one mixotroph–bacteria-only steady state e_6 if $0 < d_m < d_m^*,\ 0 < d_b < d_{b2}^*$.*

It is very difficult to obtain the existence of coexistence positive steady state e_7. The numerical simulation results indicate that e_7 exists if

$$0 < d_a < d_{a2}^*,\ \ 0 < d_m < d_{m2}^*,\ \ 0 < d_b < d_{b3}^*.$$

Model (1) can show more complex dynamic phenomena including periodic oscillations and multiple stability switches. In consideration of the motivation of the present paper, we characterize the biomass changes of autotrophs, mixotrophs and bacteria through numerical simulations and then evaluate their interactions when these three groups coexist.

From Fig. 8a, it is observed that there exist three interesting phenomena: (1) the biomass of autotrophs, mixotrophs and bacteria exhibits oscillations; (2) when the biomass of mixotrophs is relatively high, the biomass of autotrophs and bacteria is at a relatively low value; (3) the biomass of bacteria is at a low level for a long time, which

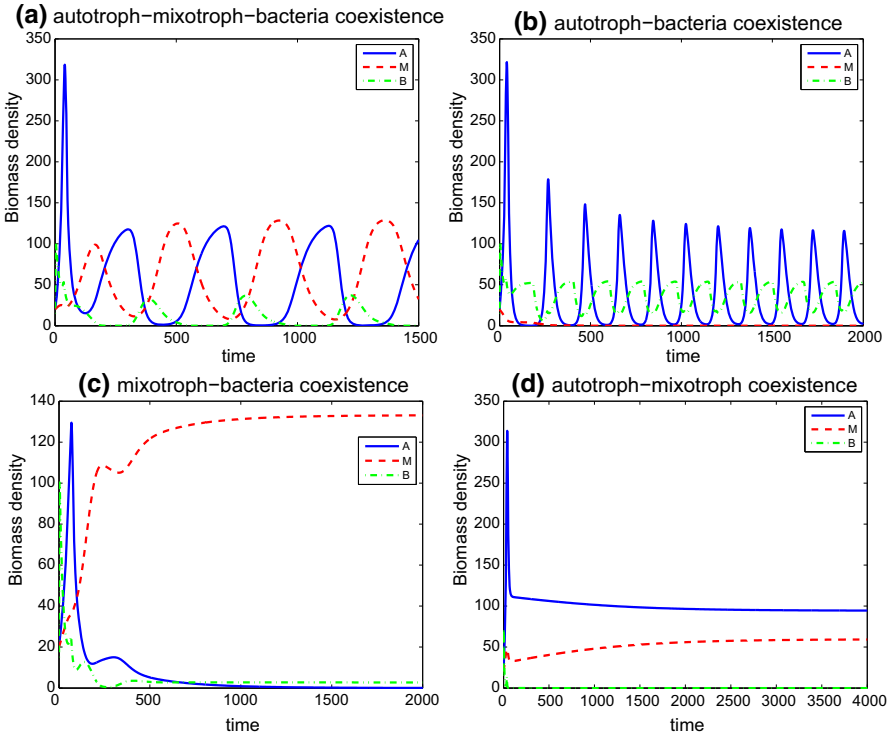

Fig. 8 The interactions between autotrophs, mixotrophs and bacteria. **a** Autotroph–mixotroph–bacteria coexistence ($d_a = 0.2, d_m = 0.27, d_b = 0.04$); **b** autotroph–bacteria coexistence ($d_a = 0.2, d_m = 0.3, d_b = 0.27$); **c** mixotroph–bacteria coexistence ($d_a = 0.25, d_m = 0.27, d_b = 0.04$); **d** autotroph–mixotroph coexistence ($d_a = 0.2, d_m = 0.25, d_b = 0.15$). Here the rest parameter values are from Table 1

means that there is a low ratio of bacterial to phytoplankton biomass. These findings are consistent with the data in La Caldera Lake from 1992 to 1999 in Medina-Sánchez et al. (2004). If mixotrophs are extinct, autotrophs and bacteria can survive, and the biomass of bacteria is higher than that of bacteria when the three coexist (see Fig. 8b). On the contrary, when mixotrophs and bacteria appear together, the biomass of bacteria is at a lower value (see Fig. 8c). This indicates that the influence of mixotrophs on the bacterial biomass is greater than that of autotrophs. Autotrophs and mixotrophs can coexist since they compete for two different resources (see Fig. 8d). Figure 8 also shows that if the phytoplankton biomass is relatively high, the bacterial biomass is at a very low value. This is because in an oligotrophic aquatic ecosystem, phytoplankton and bacteria compete for nutrients, which are an essential resource of their growth. Although the increase of phytoplankton biomass provides more organic carbon, it also consumes more nutrients. This competitive relationship causes the decrease of bacterial biomass.

These theoretical and numerical findings further confirm the statements of Medina-Sánchez, Villar-Argaiz and Carrillo in Medina-Sánchez et al. (2004). Phytoplankton containing autotrophs and mixotrophs are the main reason for the lower bacterial

biomass in La Caldera Lake. The dual control of mixotrophs on bacteria is a key factor why the biomass ratio of bacteria to phytoplankton in La Caldera Lake deviates from the traditional trend. There is a direct competition for nutrients among autotrophs, mixotrophs and bacteria. This competitive relationship is an important factor in the reduction of the bacterial biomass when the biomass of autotrophs and mixotrophs increases in an oligotrophic lake.

4 Discussion

Model (1) is proposed to describe autotroph–mixotroph–bacteria interactions based on the theory of ecological stoichiometry. Motivated by the experiments and hypotheses of Medina-Sánchez, Villar-Argaiz and Carrillo in (Medina-Sánchez et al. 2004), models (1) (3) and (8) give more detailed interpretations through theoretical analysis and numerical simulations. Our results further verify that mixotrophs are a key reason for the ratio of bacterial and phytoplankton biomass in La Caldera Lake to deviate from the general tendency. Our bifurcation diagrams (Figs. 3 and 6) show that the competition between phytoplankton and bacteria for nutrients can also be an important factor for the decrease of the bacterial biomass in an oligotrophic lake.

Model (1) is a very complex system containing multiple biological mechanisms. In the theoretical analysis, we establish the threshold conditions of phytoplankton and bacteria to invade the aquatic ecosystems for (3), (8) and (1) (see Theorems 2, 3 and 4). But there are still some remaining questions to be solved. For example, how to prove theoretically that the positive steady state of (3) or (8) will produce multiple stability switches. Due to the motivation of the present paper, we only do some simple theoretical analysis for steady state solutions of model (1). According to numerical simulation results, model (1) produce oscillations and multiple stability switches. Rigorously investigating more dynamic properties of model (1) is an interesting and important question.

Our work provides an extension of the research results in (Wang et al. 2007). Wang et al. (Wang et al. 2007) explored the interactions between bacteria and algae but without mixotrophs. They stated that an important reason for low nucleic acid (LNA) bacteria to win the competition is severely phosphorus limitation in Lake Biwa. By comparing models (3) and (8), it is found that mixotrophs have a more important impact on the bacterial biomass because of its bottom-up and top-down dual control. It is of interest to explore the role of mixotrophs in Lake Biwa, and one can expect to obtain some new insights.

Mixotrophs are widely distributed in various aquatic ecosystems, ranging from low-latitude to high-latitude lakes, rivers and oceans (Crane and Grover 2010; Edwards 2019). It effectively increases carbon fixation, transfers more organic matter to higher trophic levels, and controls the biomass of bacteria. Our study here attempts to model the interactions between autotrophs, mixotrophs and bacteria, and reveals the important role of mixotrophs in aquatic ecosystems. From the present discussion, there are more interesting biological questions that need to be further explored. For example, previous studies have shown that mixotrophs not only compete with autotrophs for resources, but also consume small autotrophic organisms (Crane and Grover 2010;

Moeller et al. 2019; Wilken et al. 2014a). They form an intraguild predation structure. In the model (1), we ignore the predation of mixotrophs on autotrophs because of the motivation of this paper. Zooplankton is also an important part of the aquatic ecological community (Loladze et al. 2000; Lv et al. 2016). The addition of zooplankton to the phytoplankton–bacteria model will produce more complex dynamic behaviors and provide new biological implications.

Author Contributions All authors contributed equally to the manuscript and typed, read and approved the final manuscript.

Declarations

Conflict of interest The authors declare that they have no conflict of interest.

Appendix

Proof of Theorem 1 Let $\Phi = AQ_a + MQ_m + qB + N$. It follows from (1) that

$$\begin{aligned}\frac{d\Phi}{dt} =& \frac{D}{L}(N_b - (AQ_a + MQ_m + qB + N)) \\ & - \left(d_a + \frac{v_a}{L}\right) AQ_a - \left(d_m + \frac{v_m}{L}\right) AQ_m - d_b q B \\ \leq& \frac{D}{L}(N_b - \Phi),\end{aligned}$$

and then $\limsup_{t\to\infty} \Phi(t) \leq N_b$. Note that $Q_{\min,a} \leq Q_a(t) \leq Q_{\max,a}$, $Q_{\min,m} \leq Q_m(t) \leq Q_{\max,m}$ for all $t \geq 0$. Then

$$\limsup_{t\to\infty} A(t) \leq \frac{N_b}{Q_{\min,a}}, \quad \limsup_{t\to\infty} M(t) \leq \frac{N_b}{Q_{\min,m}}.$$

From the last equation of (1), we have

$$\begin{aligned}\frac{dC}{dt} &\leq \mu_c(A, Q_a, M, Q_m) - \frac{D}{L}C \leq r_a A + r_m M - \frac{D}{L}C \\ &\leq \left(\frac{r_a}{Q_{\min,a}} + \frac{r_m}{Q_{\min,m}}\right) N_b - \frac{D}{L}C\end{aligned}$$

for sufficiently large t and

$$\limsup_{t\to\infty} C(t) \leq \frac{LN_b}{D}\left(\frac{r_a}{Q_{\min,a}} + \frac{r_m}{Q_{\min,m}}\right).$$

This means that the set Δ is a globally attracting region and system (1) is dissipative. □

Proof of Theorem 2 By using local bifurcation theory in (Crandall and Rabinowitz 1971), we first show that E_3 bifurcates from E_2 at $d_b = d_{b1}$. Define a mapping $F : \mathbb{R}^+ \times \mathbb{R}^5 \to \mathbb{R}^5$ by

$$F(d_b, A, Q_a, N, B, C) = \begin{pmatrix} \mu_a(A, Q_a)A - d_a A - \frac{v_a+D}{L}A \\ \rho_a(Q_a)g_a(N) - \mu_a(A, Q_a)Q_a \\ \frac{D}{L}(N_b - N) - \rho_a(Q_a)g_a(N)A - qr_b g_b(N, C)B \\ r_b g_b(N, C)B - d_b B - \frac{D}{L}B \\ \mu_c(A, Q_a) - \frac{1}{\gamma}r_b g_b(N, C)B - \frac{D}{L}C \end{pmatrix}.$$

It is easy to see that $F(d_b, A_2, Q_{a_2}, N_2, 0, C_2) = 0$. Let

$$P := F_{(A,Q_a,N,B,C)}(d_{b1}, A_2, Q_{a2}, N_2, 0, C_2).$$

For any $(\xi_1, \xi_2, \xi_3, \xi_4, \xi_5) \in \mathbb{R}^5$, we have

$$P[\xi_1, \xi_2, \xi_3, \xi_4, \xi_5] = \begin{pmatrix} p_1(\xi_1, \xi_2) \\ p_2(\xi_1, \xi_2, \xi_3) \\ p_3(\xi_1, \xi_2, \xi_3, \xi_4) \\ 0 \\ p_4(\xi_1, \xi_2, \xi_4, \xi_5) \end{pmatrix},$$

where

$$\begin{aligned}
p_1(\xi_1, \xi_2) =& \frac{\partial \mu_a}{\partial A}(A_2, Q_{a2})A_2\xi_1 + \frac{\partial \mu_a}{\partial Q_a}(A_2, Q_{a2})A_2\xi_2, \\
p_2(\xi_1, \xi_2, \xi_3) =& -\frac{\partial \mu_a}{\partial A}(A_2, Q_{a2})Q_{a2}\xi_1 + \left(\frac{\partial \rho_a}{\partial Q_a}(Q_{a2})g_a(N_2) - r_a \bar{I}_a(A_2, 0)\right)\xi_2 \\
&+ \rho_a(Q_{a2})\frac{\partial g_a}{\partial N}(N_2)\xi_3, \\
p_3(\xi_1, \xi_2, \xi_3, \xi_4) =& -\rho_a(Q_{a2})g_a(N_2)\xi_1 - \frac{\partial \rho_a}{\partial Q_a}(Q_{a2})g_a(N_2)A_2\xi_2 \\
&- \left(\frac{D}{L} + \rho_a(Q_{a2})\frac{\partial g_a}{\partial N}(N_2)A_2\right)\xi_3 - qr_b g_b(N_2, C_2)\xi_4, \\
p_4(\xi_1, \xi_2, \xi_4, \xi_5) =& \frac{\partial \mu_c}{\partial A}(A_2, Q_{a2})\xi_1 + \frac{\partial \mu_c}{\partial Q_a}(A_2, Q_{a2})\xi_2 - \frac{1}{\gamma}r_b g_b(N_2, C_2)\xi_4 - \frac{D}{L}\xi_5.
\end{aligned}$$

If $(\xi_1, \xi_2, \xi_3, \xi_4, \xi_5) \in \ker P$, then

$$\begin{aligned}
&p_1(\xi_1, \xi_2, \xi_4) = 0, \ p_2(\xi_1, \xi_2, \xi_3, \xi_4) = 0, \ p_3(\xi_1, \xi_2, \xi_3, \xi_4) = 0, \\
&p_4(\xi_1, \xi_2, \xi_4, \xi_5) = 0.
\end{aligned} \tag{A.1}$$

Let $\xi_4 = 1$, then it is clear that (A.1) has a unique solution $(\hat{\xi}_1, \hat{\xi}_2, \hat{\xi}_3, 1, \hat{\xi}_5)$. Then $\dim \ker P = 1$ and $\ker P = \text{span}\{\hat{\xi}_1, \hat{\xi}_2, \hat{\xi}_3, 1, \hat{\xi}_5\}$. It is also noted that

codim range $P = 1$ as

$$\text{range } P = \left\{(\sigma_1, \sigma_2, \sigma_3, \sigma_4, \sigma_5) \in \mathbb{R}^5 : \sigma_4 = 0\right\},$$

and

$$\begin{aligned} &P_{d_b(A,Q_a,N,B,C)}(d_{b1}, A_2, Q_{a_2}, N_2, 0, C_2)(\hat{\xi}_1, \hat{\xi}_2, \hat{\xi}_3, 1, \hat{\xi}_5) \\ &= (0, 0, 0, -1, 0) \notin \text{range } P. \end{aligned}$$

From Theorem 1.7 in (Crandall and Rabinowitz 1971), there exists a $\delta_1 > 0$ such that all positive coexistence steady states of (3) near $(d_{b1}, A_2, Q_{a_2}, N_2, 0, C_2)$ lie on a smooth curve

$$\Gamma_{ba} = \{(d_b(s), A_3(s), Q_{a3}(s), N_3(s), B_3(s), C_3(s)) : 0 < s < \delta_1\}$$

with the form

$$\begin{cases} A_3(s) = A_2 + s\hat{\xi}_1 + o(s), Q_{a3}(s) = Q_{a2} + s\hat{\xi}_2 + o(s), N_3(s) = N_2 + s\hat{\xi}_3 + o(s), \\ B_3(s) = s + o(s), C_3(s) = C_2 + s\hat{\xi}_5 + o(s). \end{cases}$$

Then part (ii) holds.

We next establish global bifurcation of positive coexistence steady states of (3). Let Υ be the set of all positive coexistence steady states of (3). It can be seen that the conditions of Theorem 3.3 and Remark 3.4 in (Shi and Wang 2009) hold. This shows that there exists a connected component Υ^+ of Υ such that it includes Γ_{ba}, and its closure contains the bifurcation point $(d_{b1}, A_2, Q_{a2}, N_2, 0, C_2)$. Moreover, Υ^+ has one of the following three cases:

(1) it is not compact in $\mathbb{R}^6$;
(2) it includes another bifurcation point $(\bar{d}_b, A_2, Q_{a2}, N_2, 0, C_2)$ with $\bar{d}_b \neq d_{b1}$;
(3) it includes a point $(d_b, A_2 + \hat{A}, Q_{a2} + \hat{Q}_a, N_2 + \hat{N}, \hat{B}, C_2 + \hat{C})$ with $0 \neq (\hat{A}, \hat{Q}_a, \hat{N}, \hat{B}, \hat{C}) \in Z$, where Z is a closed complement of ker $P = \text{span}(\hat{\xi}_1, \hat{\xi}_2, \hat{\xi}_3, 1, \hat{\xi}_5)$ in $\mathbb{R}^5$.

If the case (3) occurs, then $\hat{B} = 0$, which is a contradiction to $\hat{B} > 0$ since it is a positive steady state. Assume that the case (2) holds and $\bar{d}_b$ is another bifurcation value from Γ_a. Hence, there exists a positive coexistence steady state sequence $\{(d_b^n, A^n, Q_a^n, N^n, B^n, C^n)\}$ satisfying

$$\{(d_b^n, A^n, Q_a^n, N^n, B^n, C^n)\} \to (\bar{d}_b, A_2, Q_{a2}, N_2, 0, C_2)$$

as $n \to \infty$. From the fourth equation in (3), we have

$$r_b g_b(N^n, C^n) - d_b^n - \frac{D}{L} = 0.$$

Hence

$$r_b g_b(N_2, C_2) - \bar{d}_b - \frac{D}{L} = 0$$

when $n \to \infty$, which means that $\bar{d}_b = d_{b1}$.

The above analysis shows that the case (1) must happen. Then Υ^+ is not compact in $\mathbb{R}^6$. It follows from Theorem 1 that

$$Q_{\min,a} \le Q_{a3} \le Q_{\max,a},\ A_3 Q_{a3} + q B_3 + N_3 \le N_b,\ C_3 \le \frac{r_a L N_b}{D Q_{\min,a}}$$

for all $d_b \in (0, d_{b1})$. This indicates that the projection of Υ^+ onto d_b-axis contains $(0, d_{b1})$. This proves part (i). □

Proof of Theorem 3 (i) It is obvious that E_4 always exists. The Jacobian matrix at E_4 is

$$J(E_4) = \begin{pmatrix} a_{11} & 0 & 0 & 0 & 0 \\ a_{21} & a_{22} & a_{23} & a_{24} & 0 \\ a_{31} & 0 & a_{33} & 0 & 0 \\ 0 & 0 & 0 & a_{44} & 0 \\ a_{51} & a_{52} & 0 & a_{54} & a_{55} \end{pmatrix},$$

where

$$\begin{aligned}
&a_{11} = \mu_m(0, Q_{m4}, 0) - d_m - \frac{v_m + D}{L}, a_{21} = -\frac{\partial \mu_m}{\partial M}(0, Q_{m4}, 0) Q_{m4}, \\
&a_{22} = \frac{\partial \rho_m}{\partial Q_m}(Q_{m4}) g_m(N_b) - r_m \bar{I}_m(0,0), a_{23} = \rho_m(Q_{m4}) \frac{\partial g_m}{\partial N}(N_b), \\
&a_{24} = \frac{aq}{\delta} - \frac{\partial \mu_m}{\partial B}(0, Q_{m4}, 0) Q_{m4}, a_{31} = -\rho_m(Q_{m4}) g_m(N_b),\ a_{33} = -\frac{D}{L}, \\
&a_{44} = -d_b - \frac{D}{L}, a_{51} = \frac{\partial \mu_c}{\partial M}(0, Q_{m4}), a_{52} = \frac{\partial \mu_c}{\partial Q_m}(0, Q_{m4}), \\
&a_{54} = -\frac{r_b}{\gamma} g_b(N_b, 0), a_{55} = -\frac{D}{L}.
\end{aligned}$$

It can be observed that $J(E_4)$ has five eigenvalues a_{ii}, $i = 1, \cdots, 5$. Note that $a_{ii} < 0$ for $i = 2, 3, 4, 5$. Therefore, if $d_m > d_m^*$ holds, then $a_{11} < 0$. This means that all the five eigenvalues of $J(E_4)$ have negative real parts. This shows that E_4 is locally asymptotically stable.

(ii) The existence of E_5 is from Theorem 2 in (Wang et al. 2007). The Jacobian matrix at E_5 is

$$J(E_5) = \begin{pmatrix} a_{11} & a_{12} & 0 & a_{14} & 0 \\ a_{21} & a_{22} & a_{23} & a_{24} & 0 \\ a_{31} & a_{32} & a_{33} & a_{34} & 0 \\ 0 & 0 & 0 & a_{44} & 0 \\ a_{51} & a_{52} & 0 & a_{54} & a_{55} \end{pmatrix},$$

where

$$\begin{aligned}
a_{11} &= \frac{\partial \mu_m}{\partial M}(M_5, Q_{m5}, 0)M_5, \\
a_{12} &= \frac{\partial \mu_m}{\partial Q_m}(M_5, Q_{m5}, 0)M_5, \\
a_{14} &= \frac{\partial \mu_m}{\partial B}(M_5, Q_{m5}, 0)M_5, \\
a_{21} &= -\frac{\partial \mu_m}{\partial M}(M_5, Q_{m5}, 0)Q_{m5}, a_{22} = \frac{\partial \rho_m}{\partial Q_m}(Q_{m5})g_m(N_5) - r_m \bar{I}_m(0, M_5), \\
a_{23} &= \rho_m(Q_{m5})\frac{\partial g_m}{\partial N}(N_5), a_{24} = \frac{aq}{\delta} - \frac{\partial \mu_m}{\partial B}(M_5, Q_{m5}, 0)Q_{m5}, \\
a_{31} &= -\rho_m(Q_{m5})g_m(N_5), a_{32} = -\frac{\partial \rho_m}{\partial Q_m}(Q_{m5})g_m(N_5)M_5, \\
a_{33} &= -\frac{D}{L} - \rho_m(Q_{m5})\frac{\partial g_m}{\partial N}(N_5)M_5, a_{34} = -qr_b g_b(N_5, C_5), \\
a_{44} &= r_b g_b(N_5, C_5) - d_b - \frac{D}{L} - \frac{a}{\delta}M_5, a_{51} = \frac{\partial \mu_c}{\partial M}(M_5, Q_{m5}), \\
a_{52} &= \frac{\partial \mu_c}{\partial Q_m}(M_5, Q_{m5}), a_{54} = -\frac{r_b}{\gamma}g_b(N_5, C_5), a_{55} = -\frac{D}{L}.
\end{aligned}$$

$J(E_5)$ has eigenvalues a_{44}, a_{55}, and the remaining three eigenvalues satisfy

$$\lambda^3 + A_1\lambda^2 + A_2\lambda + A_3 = 0,$$

where

$$\begin{aligned}
A_1 &= -(a_{11} + a_{22} + a_{33}), \\
A_2 &= a_{11}a_{22} + (a_{11} + a_{22})a_{33} - (a_{23}a_{32} + a_{12}a_{21}), \\
A_3 &= -a_{11}a_{22}a_{33} - a_{12}a_{23}a_{31} + a_{11}a_{23}a_{32} + a_{12}a_{21}a_{33}.
\end{aligned}$$

A direct calculation gives $A_i > 0$, $i = 1, 2, 3$ and $A_1A_2 - A_3 > 0$. According to the Routh–Hurwitz criterion, the three eigenvalues have negative real parts. It is clear that $a_{55} < 0$. If $d_b > d_{b2}$ holds, then $a_{44} < 0$. This shows that all the five eigenvalues of $J(E_5)$ have negative real parts if $d_b > d_{b2}$ holds. Hence, E_5 is locally asymptotically stable.

(iii)-(iv) Define a mapping $G : \mathbb{R}^+ \times \mathbb{R}^5 \to \mathbb{R}^5$ by

$$G(d_b, M, Q_m, N, B, C) = \begin{pmatrix} \mu_m(M, Q_m, B)M - d_m M - \frac{v_m + D}{L} M \\ \rho_m(Q_m)g_m(N) + qf(B) - \mu_m(M, Q_m, B)Q_m \\ \frac{D}{L}(N_b - N) - \rho_m(Q_m)g_m(N)M - qr_b g_b(N, C)B \\ r_b g_b(N, C)B - d_b B - \frac{D}{L}B - f(B)M \\ \mu_c(M, Q_m) - \frac{1}{\gamma} r_b g_b(N, C)B - \frac{D}{L}C \end{pmatrix}.$$

It follows that $G(d_b, M_5, Q_{m5}, N_5, 0, C_5) = 0$. Let

$$H := G_{(M,Q_m,N,B,C)}(d_{b2}, M_5, Q_{m5}, N_5, 0, C_5).$$

For any $(\zeta_1, \zeta_2, \zeta_3, \zeta_4, \zeta_5) \in \mathbb{R}^5$, we have

$$H[\zeta_1, \zeta_2, \zeta_3, \zeta_4, \zeta_5] = \begin{pmatrix} h_1(\zeta_1, \zeta_2, \zeta_4) \\ h_2(\zeta_1, \zeta_2, \zeta_3, \zeta_4) \\ h_3(\zeta_1, \zeta_2, \zeta_3, \zeta_4) \\ 0 \\ h_4(\zeta_1, \zeta_2, \zeta_4, \zeta_5) \end{pmatrix},$$

where

$$\begin{aligned} h_1(\zeta_1, \zeta_2, \zeta_4) =& \frac{\partial \mu_m}{\partial M}(M_5, Q_{m5}, 0)M_5\zeta_1 + \frac{\partial \mu_m}{\partial Q_m}(M_5, Q_{m5}, 0)M_5\zeta_2 \\ &+ \frac{\partial \mu_m}{\partial B}(M_5, Q_{m5}, 0)M_5\zeta_4, \\ h_2(\zeta_1, \zeta_2, \zeta_3, \zeta_4) =& -\frac{\partial \mu_m}{\partial M}(M_5, Q_{m5}, 0)Q_{m5}\zeta_1 \\ &+ \left(\frac{\partial \rho_m}{\partial Q_m}(Q_{m5})g_m(N_5) - r_m \bar{I}_m(0, M_5)\right)\zeta_2 \\ &+ \rho_m(Q_{m5})\frac{\partial g_m}{\partial N}(N_5)\zeta_3 + \left(\frac{aq}{\delta} - \frac{\partial \mu_m}{\partial B}(M_5, Q_{m5}, 0)Q_{m5}\right)\zeta_4, \\ h_3(\zeta_1, \zeta_2, \zeta_3, \zeta_4) =& -\rho_m(Q_{m5})g_m(N_5)\zeta_1 - \frac{\partial \rho_m}{\partial Q_m}(Q_{m5})g_m(N_5)M_5\zeta_2 \\ &- \left(\frac{D}{L} + \rho_m(Q_{m5})\frac{\partial g_m}{\partial N}(N_5)M_5\right)\zeta_3 - qr_b g_b(N_5, C_5)\zeta_4, \\ h_4(\zeta_1, \zeta_2, \zeta_4, \zeta_5) =& \frac{\partial \mu_c}{\partial M}(M_5, Q_{m5})\zeta_1 + \frac{\partial \mu_c}{\partial Q_m}(M_5, Q_{m5})\zeta_2 - \frac{r_b}{\gamma} g_b(N_5, C_5)\zeta_4 - \frac{D}{L}\zeta_5. \end{aligned}$$

If $(\zeta_1, \zeta_2, \zeta_3, \zeta_4, \zeta_5) \in \ker H$, then

$$\begin{aligned} &h_1(\zeta_1, \zeta_2, \zeta_4) = 0,\ h_2(\zeta_1, \zeta_2, \zeta_3, \zeta_4) = 0, \\ &h_3(\zeta_1, \zeta_2, \zeta_3, \zeta_4) = 0, h_4(\zeta_1, \zeta_2, \zeta_4, \zeta_5) = 0. \end{aligned} \tag{A.2}$$

Let $\zeta_4 = 1$, then (A.2) has a unique solution $(\hat{\zeta}_1, \hat{\zeta}_2, \hat{\zeta}_3, 1, \hat{\zeta}_5)$. This implies that $\dim\ker H = 1$ and $\ker H = \text{span}\{\hat{\zeta}_1, \hat{\zeta}_2, \hat{\zeta}_3, 1, \hat{\zeta}_5\}$. It is also easy to show that $\text{codim range } H = 1$ as

$$\text{range } H = \left\{(\omega_1, \omega_2, \omega_3, \omega_4, \omega_5) \in \mathbb{R}^5 : \omega_4 = 0\right\},$$

and

$$\begin{aligned} &G_{d_b(M,Q_m,N,B,C)}(d_{b5}, M_5, Q_{m5}, N_5, 0, C_5)(\hat{\zeta}_1, \hat{\zeta}_2, \hat{\zeta}_3, 1, \hat{\zeta}_5) \\ &= (0, 0, 0, -1, 0) \notin \text{range } H. \end{aligned}$$

By using Theorem 1.7 in (Crandall and Rabinowitz 1971), there exists a $\delta_2 > 0$ such that all positive steady states of (8) near $(d_{b5}, M_5, Q_{m5}, N_5, 0, C_5)$ lie on a smooth curve

$$\Gamma_{bm} = \{(d_b(s), M_6(s), Q_{m6}(s), N_6(s), B_6(s), C_6(s)) : 0 < s < \delta_2\}$$

with the form

$$\begin{cases} M_6(s) = M_5 + s\hat{\zeta}_1 + o(s), \\ Q_{m6}(s) = Q_{m5} + s\hat{\zeta}_2 + o(s), \\ N_6(s) = N_5 + s\hat{\zeta}_3 + o(s), \\ B_6(s) = s + o(s),\ C_6(s) = C_5 + s\hat{\zeta}_5 + o(s). \end{cases}$$

This completes the proof of part (iv). Note that the proof of part (iii) is similar to those in Theorem 2. Then we omit it here. □

References

Boehrer B, Schultze M (2008) Stratification of lakes. Rev Geophys 46(2):1–27

Chang XY, Shi JP, Wang H (2021) Spatial modeling and dynamics of organic matter biodegradation in the absence or presence of bacterivorous grazing. Math Biosci 331:108501

Chen M, Fan M, Liu R, Wang XY, Yuan X, Zhu HP (2015) The dynamics of temperature and light on the growth of phytoplankton. J Theor Biol 385(21):8–19

Crandall MG, Rabinowitz PH (1971) Bifurcation from simple eigenvalues. J Funct Anal 8(2):321–340

Crane KW, Grover JP (2010) Coexistence of mixotrophs, autotrophs, and heterotrophs in planktonic microbial communities. J Theor Biol 262(3):517–527

Edwards KF (2019) Mixotrophy in nanoflagellates across environmental gradients in the ocean. Proc Natl Acad Sci USA 116(13):6211–6220

Grover JP (2003) The Impact of variable stoichiometry on predator-prey interactions: a multinutrient approach. Am Nat 162(1):29–43

Heggerud CM, Wang H, Lewis MA (2020) Transient dynamics of a stoichiometric cyanobacteria model via multiple-scale analysis. SIAM J Appl Math 80(3):1223–1246

Hsu SB, Lou Y (2010) Single phytoplankton species growth with light and advection in a water column. SIAM J Appl Math 70(8):2942–2974

Huisman J, Weissing FJ (1994) Light-limited growth and competition for light in well-mixed aquatic environments: an elementary mode. Ecology 75(2):507–520

Jiang DH, Lam KY, Lou Y, Wang ZC (2019) Monotonicity and global dynamics of a nonlocal two-species phytoplankton model. SIAM J Appl Math 79(2):716–742
Kong JD, Salceanu P, Wang H (2018) A stoichiometric organic matter decomposition model in a chemostat culture. J Math Biol 76(3):609–644
Li X, Wang H, Kuang Y (2011) Global analysis of a stoichiometric producer-grazer model with holling type functional responses. J Math Biol 63(5):901–932
Loladze I, Kuang Y, Elser JJ (2000) Stoichiometry in producer-grazer systems: linking energy flow with element cycling. Bull Math Biol 62:1137–1162
Loladze I, Kuang Y, Elser JJ, Fagan WF (2004) Competition and stoichiometry: coexistence of two predators on one prey. Theor Popul Biol 65(1):1–15
Lv DY, Fan M, Kang Y, Blanco K (2016) Modeling refuge effect of submerged macrophytes in lake system. Bull Math Biol 78(4):662–694
Medina-Sánchez JM, Villar-Argaiz M, Carrillo P (2004) Neither with nor without you: a complex algal control on bacterioplankton in a high mountain lake. Limnol Oceanogr 49(5):1722–1733
Mischaikow K, Smith H, Thieme HR (1995) Asymptotically autonomous semiflows: chain recurrence and Lyapunov functions. Trans Am Math Soc 347(5):1669–1685
Moeller HV, Neubert MG, Johnson MD (2019) Intraguild predation enables coexistence of competing phytoplankton in a well-mixed water column. Ecology 100(12):e02874
Nie H, Hsu SB, Wang FB (2019) Steady-state solutions of a reaction-diffusion system arising from intraguild predation and internal storage. J Differ Equ 266(12):8459–8491
Nie H, Hsu SB, Wang FB (2020) Global dynamics of a reaction-diffusion system with intraguild predation and internal storage. Discrete Contin Dyn Syst Ser B 25(3):877–901
Peace A, Wang H (2019) Compensatory foraging in stoichiometric producer-grazer models. Bull Math Biol 81:4932–4950
Peace A (2015) Effects of light, nutrients, and food chain length on trophic efficienciesin simple stoichiometric aquatic food chain models. Ecol Model 312:125–135
Peng R, Zhao XQ (2016) A nonlocal and periodic reaction-diffusion-advection model of a single phytoplankton species. J Math Biol 72(3):755–791
Rong X, Sun Y, Fan M, Wang H (2020) Stoichiometric modeling of aboveground-belowground interaction of herbaceous plant and two herbivores. Bull Math Biol 82:107
Shi JP, Wang XF (2009) On global bifurcation for quasilinear elliptic systems on bounded domains. J Differ Equ 246(7):2788–2812
Sterner RW, Elser JJ (2002) Ecological stoichiometry: the biology of elements from molecules to the biosphere. Princeton University Press, Princeton
Stickney HL, Hood RR, Stoecker DK (2000) The impact of mixotrophy on planktonic marine ecosystems. Ecol Model 125(2–3):203–230
Wang H, Smith HL, Kuang Y, Elser JJ (2007) Dynamics of stoichiometric bacteria-algae interactions in the epilimnion. SIAM J Appl Math 68(2):503–522
Wang H, Kuang Y, Loladze I (2008) Dynamics of a mechanistically derived stoichiometric producer-grazer model. J Biol Dyn 2(3):286–296
Wüest A, Lorke A (2003) Small-scale hydrodynamics in lakes. Annu Rev Fluid Mech 35(1):373–412
Wilken S, Verspagen JMH, Naus-Wiezer S, Van Donk E, Huisman J (2014) Comparison of predator-prey interactions with and without intraguild predation by manipulation of the nitrogen source. Oikos 123(4):423–432
Wilken S, Verspagen JMH, Naus-Wiezer S, Van Donk E, Huisman J (2014) Biological control of toxic cyanobacteria by mixotrophic predators: an experimental test of intraguild predation theory. Ecol Appl 24(5):1235–1249
Yoshiyama K, Nakajima H (2002) Catastrophic transition in vertical distributions of phytoplankton: alternative equilibria in a water column. J Theor Biol 216(4):397–408
Zhang JM, Kong JD, Shi JP, Wang H (2021) Phytoplankton competition for nutrients and light in a stratified lake: a mathematical model connecting epilimnion and hypolimnion. J Nonlinear Sci 31:35
Zhang JM, Shi JP, Chang XY (2021) A model of algal growth depending on nutrients and inorganic carbon in a poorly mixed water column. J Math Biol 83:15
Zhang JM, Shi JP, Chang XY (2018) A mathematical model of algae growth in a pelagic-benthic coupled shallow aquatic ecosystem. J Math Biol 76(5):1159–1193